Hindawi Publishing Corporation
Journal of Nanomaterials
Volume 2015, Article ID 723256, 6 pages
http://dx.doi.org/10.1155/2015/723256

Research Article

Soft-Contact Printing of Nanoparticle-Based Nanoink for Functional Nanopatterns

Ujwal Kumar Thakur,[1] Bong-Gi Kim,[2] Sang Jin Park,[1] Hyoung Won Baac,[3] Daeho Lee,[4] and Hui Joon Park[1]

[1]*Division of Energy Systems Research, Ajou University, Suwon 443-749, Republic of Korea*
[2]*Department of Organic and Nano System Engineering, Konkuk University, Seoul 143-701, Republic of Korea*
[3]*School of Electronic and Electrical Engineering, Sungkyunkwan University, Suwon 440-746, Republic of Korea*
[4]*Department of Mechanical Engineering, Gachon University, Gyeonggi-do 461-701, Republic of Korea*

Correspondence should be addressed to Hyoung Won Baac; hwbaac@skku.edu, Daeho Lee; dhl@gachon.ac.kr, and Hui Joon Park; huijoon@ajou.ac.kr

Received 22 May 2015; Accepted 2 July 2015

Academic Editor: Junyeob Yeo

A simple solution-based soft-contact printing process that could easily generate sub-100 nm nanopatterns having negligible thickness of residual layer was developed. In this process, the thickness of residual layer could be significantly decreased by controlling the concentration of nanoink or by utilizing nanoink having high curing point. Furthermore, the additional sonication process, introduced to the soft-printing process, could facilitate further decreasing the thickness of residual layer. Consequently, ZnO nanostructures having negligible residual layer were successfully fabricated, and Ag nanostructures having 63.1% average transmittance were demonstrated. We expect that our printing process can be utilized to fabricate semitransparent conductor for various optoelectronic devices by optimizing the dimensional parameters of nanopatterns.

1. Introduction

Over the last few decades, nanomanufacturing has attracted the interests of researchers due to their potential applications to various functional devices such as photovoltaic cells [1–7], sensors [8–10], lithium ion batteries [11], transistors [12, 13], resistors [14], wire-grid polarizer [15–17], and light-emitting diode (LED). Utilizing various lithography technologies like colloidal lithography [18–20], e-beam or ion beam lithography [21–24], and nanoimprint lithography (NIL) [25, 26], a variety of nanostructures could be introduced into the devices for diverse purposes. Using colloidal lithography, which utilizes the monolayer of nanoparticles as an etch mask for pattern formation, a few nanometer scale patterns can be easily accessed; however, the difficulties in controlling long range order of nanopatterns and extending them to large area format have been issues to solve. E-beam lithography also has been widely used to fabricate nanometer scale patterns for which conventional photolithography has resolution limit, but long process time and high cost have limited the application of this technology to large area high density nanostructure fabrication. Different from those technologies, NIL has shown the strong potentials as a next generation lithography technology due to its advantages such as simplicity, low cost, and high throughput in producing even a few nanometers scale high resolution patterns, making this process applicable to mass production. Though NIL was basically pattern transfer process from the nanofeatured mold to targeted resist materials when it was first invented, it has evolved into various types of NIL-applied processes until now, which can produce diverse functional periodic nanostructures.

In this work, we have demonstrated a simple soft-contact printing process for functional nanopatterns using nanoparticle- (NP-) based nanoinks. In particular, Ag and ZnO NP systems were selected for our studies due to their usefulness for various applications. For examples, Ag nanopatterns can be applicable to transparent metal electrode

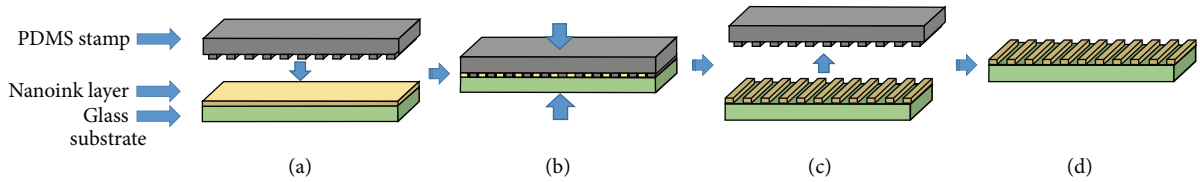

Figure 1: Nanopattern fabrication steps which include (a) covering the substrate with nanoink by PDMS stamp, (b) pressurizing and heating at proper temperature, (c) peeling off the mold after cooling down, and (d) annealing at proper temperature.

in touch screens, displays, and solar cells to improve their flexibility as a replacement of rigid indium-tin-oxide (ITO) electrode [1, 2, 27–32]. Besides, ZnO, which has direct band gap of 3.37 eV and exciton binding energy of 60 meV as a metal oxide semiconductor, is widely utilized as active layer or charge transport layer of LED, field effect transistors, sensors, batteries, and solar cells [11, 33–51]. Our results show that the resolution of our simple printing process can go down to sub-100 nm level and the residual layer of printed nanopatterns can be significantly reduced by simply changing the concentration of NP solution or controlling curing point of NP, the temperature needed to form pristine NP from solution, even without any further processes such as anisotropic etching, which is often utilized to open the residual layer after NIL. Moreover, it is shown that sonication-assisted printing process, introduced in our work, is helpful to further decrease the thickness of residual layer.

2. Materials and Methods

2.1. Nanoparticle Preparation. ZnO NP ink was prepared according to the previous publication [52]. 4.46 mM of zinc acetate ($Zn(O_2CCH_3)_2$) and 0.25 mL of water were added into a flask containing 42 mL of methanol followed by vigorous stirring at 60°C until zinc acetate was fully dissolved. In another flask, 7.22 mM of potassium hydroxide (KOH) was dissolved in 23 mL methanol. Then, the potassium hydroxide solution was dropped into the zinc acetate solution within 10–15 min while minimizing temperature fluctuation. 6 nm diameter ZnO NPs were produced after maintaining the temperature of mixture solution at 60°C for 2 h and 15 min with vigorous stirring. Since as-synthesized NPs are not fully dispersed in the methanol solution, postprocessing is required. The NP solution was centrifuged for 15 min to separate the NPs from the solvent. After discarding the solvent, 1-pentanol ($CH_3(CH_2)_4OH$) was added to produce 5 wt%, 7.5 wt%, and 11 wt% ZnO NP ink and sonicated for 1 hour. As for Ag nanoparticle, DGP 40LT-15C (curing point: 120–150°C), denoted as low curing point Ag (LCP Ag) hereafter, and DGP 45HTG (curing point: 400–550°C), denoted as high curing point Ag (HCP Ag) hereafter, having different boiling points, were purchased from Advanced Nano Products and utilized for nanopattern formation.

2.2. PDMS Stamp Preparation. Polydimethylsiloxane (PDMS) mold was prepared as described in previous publication [1]. Polymer resist template (MRI-8030, Microresist Technology GmbH) was prepared by using NIL technique using proper SiO_2 mold having 700 nm period. The PDMS stamp was fabricated by replicating imprinted polymer resist template. PDMS stamp was prepared by two different types of PDMS materials. High modulus PDMS [53] was firstly casted on polymer resist template and cured at 65°C for 5 min. Then, another PDMS (Sylgard-184 Dow corning) was drop-casted and cured at 65°C for 4 h on high modulus PDMS layer to provide the flexible mechanical support to the patterned layer.

2.3. Printing Process. Figure 1 illustrates the patterning procedures of ZnO and Ag NPs by using soft PDMS stamp. In the first step, a few drops of ZnO or Ag NP were dropped on the substrate and covered by previously prepared PDMS stamp. Those samples were pressed for 1 hour with approximately 1 bar pressure and the annealing temperatures were 130°C for ZnO and 150°C for Ag nanoink, respectively. The stamp was then peeled off and the substrate with ZnO nanopatterns was annealed at 170°C for 10 min and then cooled down at room temperature. Meanwhile, substrates with Ag nanopatterns were heated at 200°C for 2 h to check the variation in transmittance.

3. Results and Discussion

SEM images of ZnO nanopatterns, fabricated by soft-contact printing on glass substrates, are represented in Figure 2, and it is clearly shown that sub-100 nm scale nanopatterns can be successfully fabricated using this process. The thickness of residual layer is one of the most important parameters in NIL, needed to be considered to extend the applicability of the resultant nanostructures. To control the thickness of residual layer, the effect of NP concentration on the thickness of residual layer was investigated, first. The concentration of NP was changed from 11% to 5.5%, and it was found that the thickness of residual layer significantly decreased and reached negligible level at the concentration of 5.5% (Figures 2(a) and 2(b)). Nanopatterns fabricated by ZnO nanoink with 11 wt% concentration have about 670 nm thick residual layer, and it decreased to about 130 nm at 7.5% concentration, consequently almost disappearing at 5.5% concentration.

The thickness of residual layer could decrease by applying sonication process during the printing. ZnO nanoink was printed by PDMS stamp and then immediately sonicated in deionized water to provide better scattering of NPs, which were trapped between stamp and substrate. After 3 min of sonication, the pressurized stamp and substrate samples were heated at 130°C and the same procedure, described in Figure 1, was followed. Figure 3 shows the SEM image of

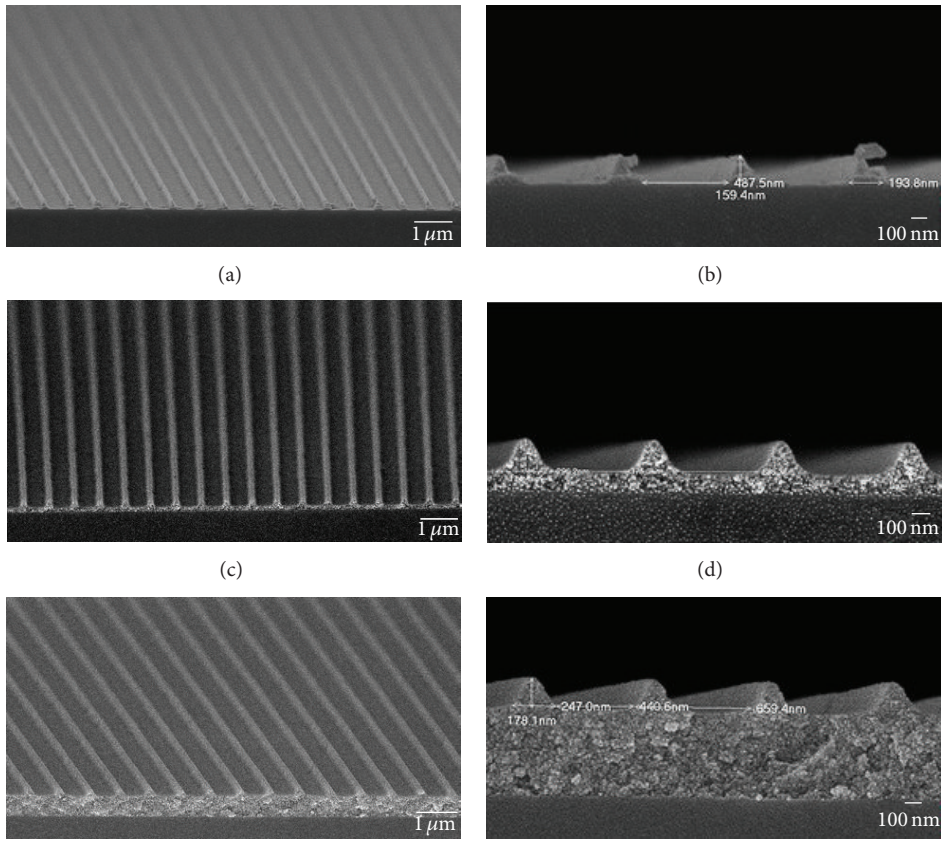

Figure 2: Tilt and cross-sectional view of nanopatterns fabricated by ZnO nanoink having ((a), (b)) 5.5%, ((c), (d)) 7.5%, and ((e), (f)) 11% concentration. The residual layer of nanopattern fabricated by nanoink having the concentration of 11% is the thickest about 670 nm, while that of nanopattern fabricated by nanoink having the concentration of 5% is the thinnest (less than 10 nm). The thickness of residual layer fabricated by ZnO nanoink with the concentration of 7.5% is about 130 nm.

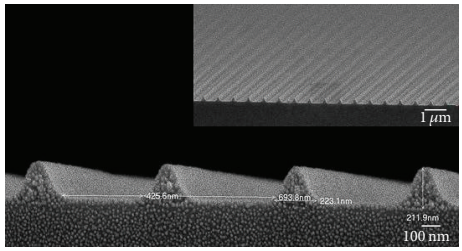

Figure 3: Effect of sonication on ZnO nanopatterns fabricated by nanoink with ZnO concentration of 7.5%. The patterns have negligible residual layer.

nanopatterns fabricated by nanoink having the concentration of 7.5 wt%, which gives around 130 nm thickness of residual layer without sonication, showing negligible residual layer thickness with sonication process.

The effect of NP curing temperature on the residual layer was investigated by Ag NP solutions. For this purpose, two types of Ag nanoinks having different curing temperature, LCP Ag and HCP Ag, were utilized, and Ag nanopatterns were prepared by similar process, depicted in Figure 1. Nanoinks were firstly filtered by 0.45 μm syringe filter to remove impurities and the filtered nanoinks were dispensed over the UV-treated glass substrate to improve wettability of solution. After printing them with a PDMS stamp, the substrate was also heated at 150°C for 1 hour. After cooling them down to room temperature finally the stamp was peeled off. The SEM images of the resultant nanopatterns are shown in Figure 4, and it is clearly shown that almost residual layer-free nanopatterns can be achieved using HCP Ag NP solution (Figure 4a). It is expected that HCP Ag NP, which can have enough time for them to be assembled due to their high curing temperature, is advantageous to eliminating Ag NP in the residual layer position.

After peeling off the PDMS stamp the nanopatterns ware annealed at 200°C for 2 h, and their transmittance was measured. It was found that the transmittance of Ag nanopatterns from HCT Ag was significantly improved from 46.1% to 63.1% on an average in the range of 400 nm to 800 nm after annealing; however, that from LCT Ag was almost similar even after further annealing (from 41.0% to 43.5% on an average). This may be because Ag NPs, prepared by LCT Ag, are randomly scattered in the trench of nanogratings (Figures 4(b1) and 4(b2)) and those cannot

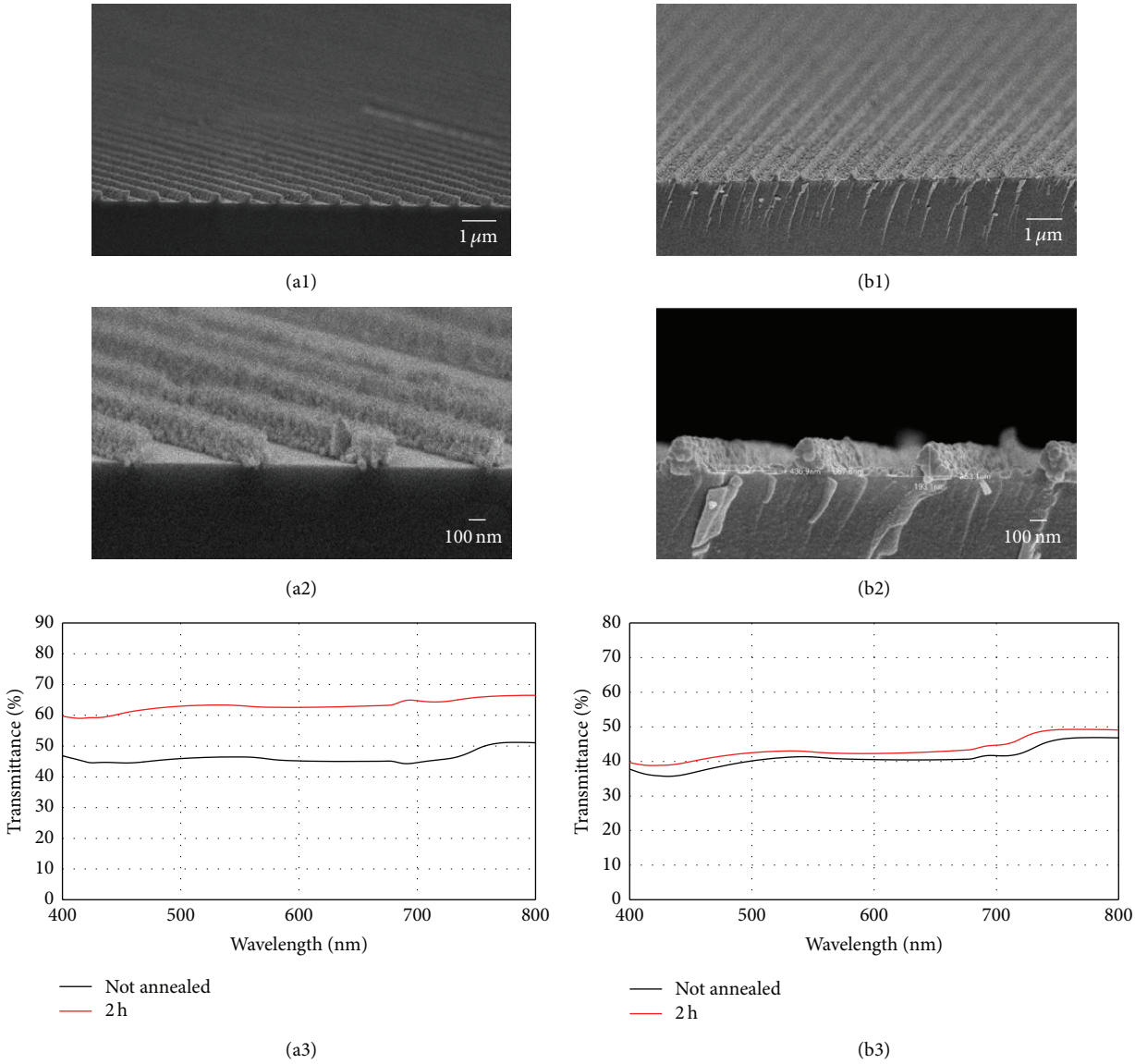

FIGURE 4: Tilted (a1) and cross-sectional (a2) view of Ag nanopattern fabricated by HCP Ag nanoink. Tilted (b1) and cross-sectional (b2) view of Ag nanopattern fabricated by Ag LCP nanoink. Transmittance of nanopatterns fabricated by Ag HCP nanoink (a3) and Ag LCP nanoink (b3).

be efficiently assembled to improve their transmittance after annealing. Different from this, Ag NPs, fabricated by HCT Ag, already formed nanograting structure almost without residual layer (Figures 4(a1) and 4(a2)) and therefore could be efficiently assembled to give more narrow line width during annealing, improving their transmittance.

4. Summary

The residual layer in ZnO nanopatterns could be tuned by controlling the concentration of ZnO nanoink. ZnO nanopatterns having negligible residual layer could be prepared by using ZnO nanoink with the concentration of 5.5%. Furthermore, it was shown that the additional sonication process, introduced to our soft-printing process, could facilitate decreasing the thickness of residual layer of nanopatterns. The effect of evaporation of solvent in nanoink solution on the residual layer of nanopatterns was also investigated. Ag nanopatterns having negligible residual layer were successfully fabricated by utilizing Ag nanoink that had higher curing temperature, and the average transmittance of the resultant Ag nanopatterns could approach 63.1%. It is expected that our approach can be a promising way to prepare semitransparent conductor by further optimizing dimensional parameters of nanopattern, such as width and height of nanostructure, consequently improving the transmittance.

Conflict of Interests

The authors declare that there is no conflict of interests regarding the publication of this paper.

Authors' Contribution

Ujwal Kumar Thakur and Bong-Gi Kim have equally contributed to this work.

Acknowledgments

Hui Joon Park acknowledges the support by the Basic Science Research Program through the National Research Foundation of Korea (NRF) funded by the Ministry of Education (2014R1A1A2056403). Daeho Lee acknowledges the support by Gachon University Research Fund of 2014 (GCU-2014-0107). Hyoung Won Baac acknowledges the support from the Basic Science Research Program through the National Research Foundation of Korea funded by the Ministry of Education (NRF-2014R1A1A2059612).

References

[1] M.-G. Kang, H. Joon Park, S. Hyun Ahn, and L. Jay Guo, "Transparent Cu nanowire mesh electrode on flexible substrates fabricated by transfer printing and its application in organic solar cells," *Solar Energy Materials and Solar Cells*, vol. 94, no. 6, pp. 1179–1184, 2010.

[2] M. G. Kang, M. S. Kim, L. J. Guo et al., "Organic solar cells using nanoimprinted transparent metal electrodes," *Advanced Materials*, vol. 20, pp. 4408–4413, 2008.

[3] M.-G. Kang, T. Xu, H. J. Park, X. Luo, and L. J. Guo, "Efficiency enhancement of organic solar cells using transparent plasmonic Ag nanowire electrodes," *Advanced Materials*, vol. 22, no. 39, pp. 4378–4383, 2010.

[4] M.-G. Kang, H. J. Park, S. H. Ahn, T. Xu, and L. J. Guo, "Toward low-cost, high-efficiency, and scalable organic solar cells with transparent metal electrode and improved domain morphology," *IEEE Journal on Selected Topics in Quantum Electronics*, vol. 16, no. 6, pp. 1807–1820, 2010.

[5] S. R. Forrest, "The path to ubiquitous and low-cost organic electronic appliances on plastic," *Nature*, vol. 428, no. 6986, pp. 911–918, 2004.

[6] H. Youn, H. J. Park, and L. J. Guo, "Printed nanostructures for organic photovoltaic cells and solution-processed polymer light-emitting diodes," *Energy Technology*, vol. 3, no. 4, pp. 340–350, 2015.

[7] H. J. Park, T. Xu, J. Y. Lee, A. Ledbetter, and L. J. Guo, "Photonic color filters integrated with organic solar cells for energy harvesting," *ACS Nano*, vol. 5, no. 9, pp. 7055–7060, 2011.

[8] H. Ko, S. Singamaneni, and V. V. Tsukruk, "Nanostructured surfaces and assemblies as SERS media," *Small*, vol. 4, no. 10, pp. 1576–1599, 2008.

[9] R. A. Tripp, R. A. Dluhy, and Y. Zhao, "Novel nanostructures for SERS biosensing," *Nano Today*, vol. 3, no. 3-4, pp. 31–37, 2008.

[10] T.-P. Chen, S.-P. Chang, F.-Y. Hung, S.-J. Chang, Z.-S. Hu, and K.-J. Chen, "Simple fabrication process for 2D ZnO nanowalls and their potential application as a methane sensor," *Sensors*, vol. 13, no. 3, pp. 3941–3950, 2013.

[11] Z. Wu, L. Qin, and Q. Pan, "Fabrication and electrochemical behavior of flower-like ZnO-CoO-C nanowall arrays as anodes for lithium-ion batteries," *Journal of Alloys and Compounds*, vol. 509, no. 37, pp. 9207–9213, 2011.

[12] S. M. Sultan, N. J. Ditshego, R. Gunn, P. Ashburn, and H. M. Chong, "Effect of atomic layer deposition temperature on the performance of top-down ZnO nanowire transistors," *Nanoscale Research Letters*, vol. 9, article 517, 2014.

[13] M. Ikawa, T. Yamada, H. Matsui et al., "Simple push coating of polymer thin-film transistors," *Nature Communications*, vol. 3, pp. 1176–1183, 2012.

[14] S. H. Ko, I. Park, H. Pan et al., "Direct nanoimprinting of metal nanoparticles for nanoscale electronics fabrication," *Nano Letters*, vol. 7, no. 7, pp. 1869–1877, 2007.

[15] F. Meng, G. Luo, I. Maximov, L. Montelius, J. Chu, and H. Xu, "Fabrication and characterization of bilayer metal wire-grid polarizer using nanoimprint lithography on flexible plastic substrate," *Microelectronic Engineering*, vol. 88, no. 10, pp. 3108–3112, 2011.

[16] K. S. Park, J. M. Dang, M. M. Sung, and S.-M. Seo, "One-step fabrication of nanowire-grid polarizers using liquid-bridge-mediated nanotransfer molding," *Nanoscale Research Letters*, vol. 7, pp. 351–355, 2012.

[17] Y. J. Shin, C. Pina-Hernandez, Y.-K. Wu, J. G. Ok, and L. J. Guo, "Facile route of flexible wire grid polarizer fabrication by angled-evaporations of aluminum on two sidewalls of an imprinted nanograting," *Nanotechnology*, vol. 23, no. 34, Article ID 344018, 2012.

[18] B. Ai, Y. Yu, H. Möhwald, G. Zhang, and B. Yang, "Plasmonic films based on colloidal lithography," *Advances in Colloid and Interface Science*, vol. 206, pp. 5–16, 2014.

[19] M. A. Wood, "Colloidal lithography and current fabrication techniques producing in-plane nanotopography for biological applications," *Journal of the Royal Society Interface*, vol. 4, no. 12, pp. 1–17, 2007.

[20] S.-M. Yang, S. G. Jang, D.-G. Choi, S. Kim, and H. K. Yu, "Nanomachining by colloidal lithography," *Small*, vol. 2, no. 4, pp. 458–475, 2006.

[21] W. Hu, K. Sarveswaran, M. Lieberman, and G. H. Bernstein, "Sub-10 nm electron beam lithography using cold development of poly(methylmethacrylate)," *Journal of Vacuum Science & Technology B: Microelectronics and Nanometer Structures*, vol. 22, no. 4, pp. 1711–1716, 2004.

[22] V. Nandwana, C. Subramani, Y.-C. Yeh et al., "Direct patterning of quantum dot nanostructures via electron beam lithography," *Journal of Materials Chemistry*, vol. 21, no. 42, pp. 16859–16862, 2011.

[23] A. Joshi-Imre and S. Bauerdick, "Direct-write ion beam lithography," *Journal of Nanotechnology*, vol. 2014, Article ID 170415, 26 pages, 2014.

[24] C. M. Kolodziej and H. D. Maynard, "Electron-beam lithography for patterning biomolecules at the micron and nanometer scale," *Chemistry of Materials*, vol. 24, no. 5, pp. 774–780, 2012.

[25] S. Y. Chou, P. R. Krauss, and P. J. Renstrom, "Nanoimprint lithography," *Journal of Vacuum Science & Technology B*, vol. 14, no. 6, pp. 4129–4133, 1996.

[26] J. G. Ok, Y. J. Shin, H. J. Park, and L. J. Guo, "A step toward next-generation nanoimprint lithography: extending productivity and applicability," *Applied Physics A*, 2015.

[27] S.-E. Park, S. Kim, D.-Y. Lee, E. Kim, and J. Hwang, "Fabrication of silver nanowire transparent electrodes using electrohydrodynamic spray deposition for flexible organic solar cells," *Journal of Materials Chemistry A*, vol. 1, no. 45, pp. 14286–14293, 2013.

[28] C.-H. Liu and X. Yu, "Silver nanowire-based transparent, flexible, and conductive thin film," *Nanoscale Research Letters*, vol. 6, article 75, 2011.

[29] J.-W. Liu, J.-L. Wang, Z.-H. Wang, W.-R. Huang, and S.-H. Yu, "Manipulating nanowire assembly for flexible transparent electrodes," *Angewandte Chemie International Edition*, vol. 53, no. 49, pp. 13477–13482, 2014.

[30] J. Park and J. Hwang, "Fabrication of a flexible Ag-grid transparent electrode using ac based electrohydrodynamic Jet printing," *Journal of Physics D: Applied Physics*, vol. 47, no. 40, Article ID 405102, 2014.

[31] Y.-H. Shin, C.-K. Cho, and H.-K. Kim, "Resistance and transparency tunable Ag-inserted transparent InZnO films for capacitive touch screen panels," *Thin Solid Films*, vol. 548, pp. 641–645, 2013.

[32] J. Lee, P. Lee, H. Lee, D. Lee, S. S. Lee, and S. H. Ko, "Very long Ag nanowire synthesis and its application in a highly transparent, conductive and flexible metal electrode touch panel," *Nanoscale*, vol. 4, no. 20, pp. 6408–6414, 2012.

[33] Y.-S. Choi, J.-W. Kang, D.-K. Hwang, and S.-J. Park, "Recent advances in ZnO-based light-emitting diodes," *IEEE Transactions on Electron Devices*, vol. 57, no. 1, pp. 26–41, 2010.

[34] J.-H. Lim, K. H. Lee, and D. C. Lim, "ZnO light emitting diodes using ZnO quantum dots embedded in an amorphous silicon-oxide matrix," *Journal of the Korean Physical Society*, vol. 58, no. 6, pp. 1664–1667, 2011.

[35] S. M. Chou, L. G. Teoh, W. H. Lai, Y. H. Su, and M. H. Hon, "ZnO:Al thin film gas sensor for detection of ethanol vapor," *Sensors*, vol. 6, no. 10, pp. 1420–1427, 2006.

[36] D. Liu, M. K. Gangishetty, and T. L. Kelly, "Effect of $CH_3NH_3PbI_3$ thickness on device efficiency in planar heterojunction perovskite solar cells," *Journal of Materials Chemistry A*, vol. 2, no. 46, pp. 19873–19881, 2014.

[37] M. H. Kumar, N. Yantara, S. Dharani et al., "Flexible, low-temperature, solution processed ZnO-based perovskite solid state solar cells," *Chemical Communications*, vol. 49, no. 94, pp. 11089–11091, 2013.

[38] K. Hwang, Y.-S. Jung, Y.-J. Heo et al., "Toward large scale roll-to-roll production of fully printed perovskite solar cells," *Advanced Materials*, vol. 27, no. 7, pp. 1241–1247, 2015.

[39] J. Kim, G. Kim, T. K. Kim et al., "Efficient planar-heterojunction perovskite solar cells achieved via interfacial modification of a sol–gel ZnO electron collection layer," *Journal of Materials Chemistry A*, vol. 2, no. 41, pp. 17291–17296, 2014.

[40] F. J. Ramos, M. C. Lõpez-Santos, E. Guillén et al., "Perovskite solar cells based on nanocolumnar plasma-deposited ZnO thin films," *ChemPhysChem*, vol. 15, no. 6, pp. 1148–1153, 2014.

[41] M. Nijland, A. George, S. Thomas et al., "Patterning of epitaxial perovskites from micro and nano molded stencil masks," *Advanced Functional Materials*, vol. 24, pp. 6853–6861, 2014.

[42] O. Lupan, L. Chow, S. Shishiyanu et al., "Nanostructured zinc oxide films synthesized by successive chemical solution deposition for gas sensor applications," *Materials Research Bulletin*, vol. 44, no. 1, pp. 63–69, 2009.

[43] Q. Zhou, W. Chen, L. Xu, and S. Peng, "Hydrothermal synthesis of various hierarchical ZnO nanostructures and their methane sensing properties," *Sensors*, vol. 13, no. 5, pp. 6171–6182, 2013.

[44] P. Fei, P.-H. Yeh, J. Zhou et al., "Piezoelectric potential gated field-effect transistor based on a free-standing ZnO wire," *Nano Letters*, vol. 9, no. 10, pp. 3435–3439, 2009.

[45] E.-J. Yun, Y.-W. Song, H. G. Nam, N.-I. Cho, and M. Jung, "Development of ZnO thin film transistors based on SiN/Al_2O_3 gate dielectric materials," *Journal of the Korean Physical Society*, vol. 58, no. 3, pp. 487–491, 2011.

[46] P. C. Chang, Z. Fan, C. J. Chien, D. Stichteonth, C. Ronning, and J. G. Lu, "High-performance ZnO nanowire field effect transistors," *Applied Physics Letters*, vol. 89, Article ID 133113, 3 pages, 2006.

[47] C. Opoku, K. F. Hoettges, M. P. Hughes, V. Stolojan, S. R. P. Silva, and M. Shkunov, "Solution processable multi-channel ZnO nanowire field-effect transistors with organic gate dielectric," *Nanotechnology*, vol. 24, no. 40, Article ID 405203, 2013.

[48] S. Ju, K. Lee, D. B. Janes, M.-H. Yoon, A. Facchetti, and T. J. Marks, "Low operating voltage single ZnO nanowire field-effect transistors enabled by self-assembled organic gate nanodielectrics," *Nano Letters*, vol. 5, no. 11, pp. 2281–2286, 2005.

[49] K. Cheng, Q. Li, J. Meng et al., "Interface engineering for efficient charge collection in Cu_2O/ZnO heterojunction solar cells with ordered ZnO cavity-like nanopatterns," *Solar Energy Materials & Solar Cells*, vol. 116, pp. 120–125, 2013.

[50] L. Wang, Y. Kang, X. Liu, S. Zhang, W. Huang, and S. Wang, "ZnO nanorod gas sensor for ethanol detection," *Sensors and Actuators, B: Chemical*, vol. 162, no. 1, pp. 237–243, 2012.

[51] M. Willander, O. Nur, S. Zaman, A. Zainelabdin, N. Bano, and I. Hussain, "Zinc oxide nanorods/polymer hybrid heterojunctions for white light emitting diodes," *Journal of Physics D: Applied Physics*, vol. 44, no. 22, Article ID 224017, 2011.

[52] D. Lee, H. Pan, S. H. Ko, H. K. Park, E. Kim, and C. P. Grigoropoulos, "Non-vacuum, single-step conductive transparent ZnO patterning by ultra-short pulsed laser annealing of solution-deposited nanoparticles," *Applied Physics A: Materials Science and Processing*, vol. 107, no. 1, pp. 161–171, 2012.

[53] C. Pina-Hernandez, J.-S. Kim, L. J. Guo, and P.-F. Fu, "High-throughput and etch-selective nanoimprinting and stamping based on fast-thermal-curing poly(dimethylsiloxane)s," *Advanced Materials*, vol. 19, no. 9, pp. 1222–1227, 2007.